2018

Performance Analysis On A Variable Capacity Swash Plate Compressor

Jae Woong Choi
Incheon National University, Korea, 625gi@naver.com

Jeong Taek Lim
Incheon National University, Korea, 92_52@naver.com

Young Jae Noh
Incheon National University, Korea, youngjae427@naver.com

Hyun-Jin Kim
Incheon National University, hjkim@inu.ac.kr

Pil Gon Song
Hanon Systems, Korea, psong1@hanonsystems.com

See next page for additional authors

Authors
Jae Woong Choi, Jeong Taek Lim, Young Jae Noh, Hyun-Jin Kim, Pil Gon Song, and Seong-Min Pae

Performance analysis on a variable capacity swash plate compressor

Jae-Woong Choi[1], Jeong-Taek Lim[1] , Young-Jae Noh[1] , Hyun-Jin Kim[1]*,
Pil-Gon Song[2], Seong-Min Pae[2]

[1]Department of Mechanical Engineering, Incheon National University, Incheon, Korea
Tel : +82-32-835-8419, Fax +81-32-835-0793, E-mail: hjkim@inu.ac.kr

[2]CAE Team, Hanon Systems, Daejeon, Korea
Tel : +82-42-930-6768, E-mail: PSONG1@hanonsystems.com

* Corresponding Author

ABSTRACT

A numerical study on the performance of a variable capacity swash plate compressor for an automotive air-conditioning system was carried out. The compressor under investigation had six cylinders and capacity regulation was made by changing the swash plate inclination angle. A numerical simulation program was made based on mathematical modelings on the swash plate dynamics, refrigerant states in various control volumes such as cylinders and crank room, and flows in the opening passages of electric control valve for crank room pressure control. The simulation results such as mass flow rate, compressor power consumption, cooling capacity and COP were compared with measurements within ±5% deviation over various operating conditions except at low operating speed such as idling condition. By using the simulation program, the effect of the crank room pressure on the swash plate inclination angle and the determination of the crank room pressure level by the electric control valve openings could be investigated.

1. INTRODUCTION

Wobble plate type or swash plate type compressors are the most popular compressors for engine-driven mobile air-conditioning systems. For such wobble-plate type and swash plate-type compressors, the nutating motion of the wobble plate or swash plate produces reciprocating motion in a direction parallel to the centerline of the rotating driveshaft, and cooling capacity is determined by piston stroke for given compressor speed.
For compressors with fixed inclination plate angle, piston stroke is also fixed and the cooling capacity of the compressors changes only with engine operating speed. The cooling load for the compartment can only be controlled by on-off control of compressor clutch attachment to the engine shaft. Such on-off control causes abrupt changes to the engine torque, affecting drivability and fuel energy consumption. In addition to these shortcomings, reliability and durability can be improved by modulating the cooling capacity in a continuous manner rather than in on-off manner. Continuous modulation of the cooling capacity can be achieved by adopting mechanism of varying piston stroke continuously. The piston stroke change can be made by changing the inclination angle of the wobble or swash plate. Control of the inclination angle of the wobble or swash plate is carried out through the complicated dynamic motion of many related components inside the compressor. Among many forces and moments acting on the inclined plate, the pressure in the crank room, where inclined wobble or swash plate is exposed, plays a key role in producing the moment to change the plate inclination.

In open literatures, several analytical studies were found on the dynamic behavior of the variable stroke nutating plate together with related pistons, rotating journal and driving shaft for swash plate type [4-7], and wobble plate type compressors [1-3]. For a six-cylinder variable-displacement wobble-plate compressor, the complicated motion of each moving element of the compressor was thoroughly analyzed from both kinematic and dynamic viewpoints

[3]. An analytical model for evaluating the dynamic behavior of variable stroke wobble plate compressors was developed and applied to a sample variable displacement compressor for some practical design guides [1].

The nonlinear dynamics of the variable stroke swash plate mechanism was investigated, and constraint-induced dynamic instability was characterized [4]. For a variable displacement swash plate compressor, Tian et al.[6] developed a mathematical model of the flow control valve which control the crank room pressure to change the swash plate inclination. A study on the internal control valve could also be found in Lee and Lee [9]. Steady-state mathematical model of a variable displacement swash plate compressor was developed by combining models of the flow control valve, the dynamics of moving elements such as pistons and swash plate, and compression process model [5]. However, the compression process model was obtained by fitting the data from experiments instead of analytical modeling.

While many works are found on the dynamics of the inclined rotating plate together with associated moving elements, on the flow control valves to control piston stroke, and on the gas compression, works on the combined modeling of these individual analytical modules for a variable displacement swash plate compressor are rare in the open literature.

In this study, a detailed analysis of a variable displacement swash plate-type compressor is performed with a particular focus on the variable stroke performance.

2. Swash plate compressor with variable stroke

2.1 Compressor model

Fig. 1 shows a schematic cross-section of a swash plate compressor with variable stroke, and the compressor specifications are given in Table 1.

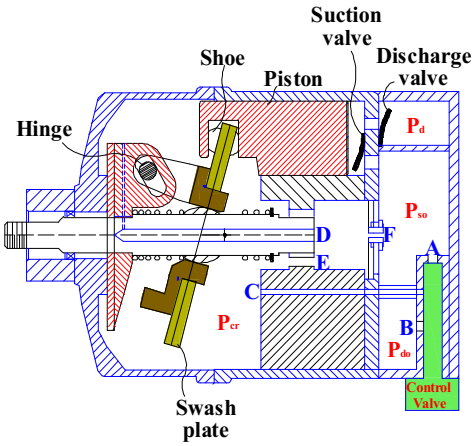

Figure 1: Schematic view of variable displacement swash plate compressor

Table 1: Swash plate compressor specifications

Compressor type	Swash plate type
Number of pistons	6
Cylinder bore	33.93 [mm]
Swash plate angle	0.55~21.8 [deg.]
Stroke, max	31.96 [mm]
Displacement volume	160 [cc]
Refrigerant	R134a

It consists of six pistons mounted along the circumference of the inclined swash plate with piston shoes in between. The rotating motion of the swash plate makes the pistons move in a reciprocating manner parallel to the shaft. Pressure-actuated reed type valves are situated on the suction and discharge ports at each cylinder head. Gas discharged from each cylinder is collected in the discharge manifold and finally discharged out of the compressor.
On the suction side, the refrigerant enters into the suction manifold located at the central portion of the compressor head to be distributed into the cylinders one by one as the swash plate rotates.

2.2 Electric control valve and swash plate angle control

The inclination angle of the swash plate is determined by the moment balance acting on the swash plate. Fig.2 shows various pitching moments acting on the swash plate. Moments due to cylinder gas forces on the pistons and piston inertia make the swash plate incline more, while those due to crank room pressure, plate centrifugal, and spring restoring forces act to reduce the swash plate inclination angle. Among these factors of affecting the pitching moment, the crank room pressure can be used for active control of the swash plate inclination: reduction of the crank room pressure causes decrease of the pitching moment on the swash plate so that the swash plate inclination is reduced.

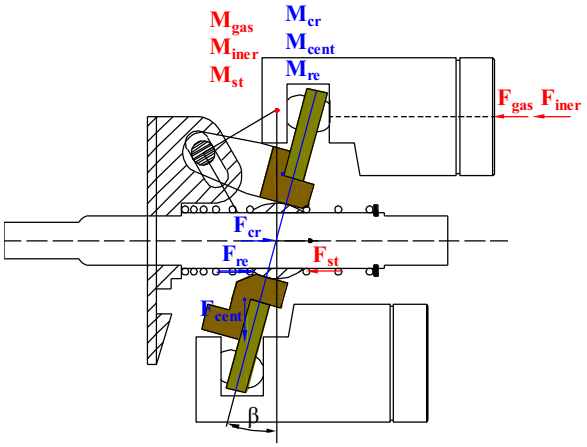

Figure 2: Pitching moment acting on the swash plate

The control of the crank room pressure is made by the electric control valve (ECV). Electromagnetic force on the valve plunger is produced by electric current input and the valve plunger movement determines selective opening among suction manifold(A), discharge manifold(B), and crank room(C) and also the degree of opening area.

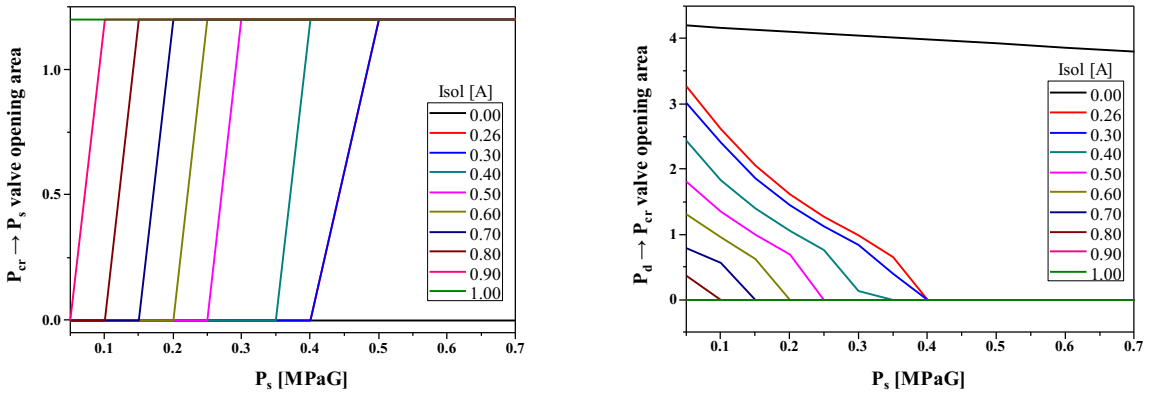

(a) (b)

Figure 3: Flow control valve (a) opening of P_{cr} to P_s (b) opening of P_d to P_{cr}

Fig.3(a) shows variation of openings in ECV flow passages with electric input. To increase the crank room pressure for reducing the swash plate inclination angle, the valve plunger is made to move for opening between B and C so that discharge pressure gas is allowed to flow into the crank room. On the other hand, reduction of the crank room pressure to increase the swash plate inclination angle can be attained when opening between C and A is made, while closing between B and C.

3. Performance analysis

3.1 Basic structure of mathematical model

Fig.4 shows a schematic of basic structure of mathematical model for performance analysis of a variable stroke swash plate compressor. For given operating conditions of suction pressure P_s, discharge pressure P_d, and shaft speed N together with preset ECV opening area, cylinder pressures ($P_{c,i}$) are calculated as a function of the crank angle. The crank room pressure P_{cr} is determined by in/out flows from/to ECV openings and also by cylinder leak flows and flow out through an orifice between the crank room and the suction manifold. Cylinder pressures and crank room pressure are to determine the swash plate angle which, in turn, affects the piston stroke for the gas compression in the cylinders, resulting in the cooling capacity.

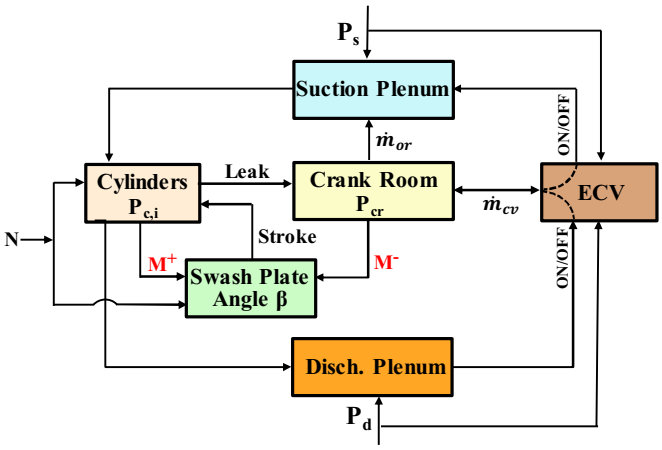

Figure 4: Control of piston stroke by swash plate angle

3.2 Gas pressure

For gas pressure calculation, control volumes to be considered are six cylinders, suction and discharge manifolds, and the crank room.

Piston stroke and related cylinder volume are given by equations (1) and (2), respectively.

$$z_i = R_c \cdot \tan(\beta) \cdot (1 - \cos(\theta_i(t))) \quad , \quad V_i(t) = z_i \cdot A_c \qquad (1),(2)$$

The mass of a cylinder is obtained by equation (3).

$$M_{c,i}(t) = M_{c,i}(0) - \int^t \{\dot{m}_{dv}(t) - \dot{m}_{sv}(t) + \dot{m}_{lk}(t)\} dt \qquad (3)$$

Gas density is then calculated by equation (4). Once gas density and entropy are given, pressure and temperature are obtained by the formulated database of REFPROP 7.0 as in equations (5a) and (5b), respectively. As for entropy, the average value during the compression process is used.

$$\rho_c = \frac{M_c(t)}{V_i(t)} \quad , \quad P=P(\rho,s) \quad , \quad T=T(\rho,s) \qquad (4),(5a),(5b)$$

Gas pressures at other chambers are obtained in a similar manner. Fig. 5 contains a cylinder pressure diagram for all.

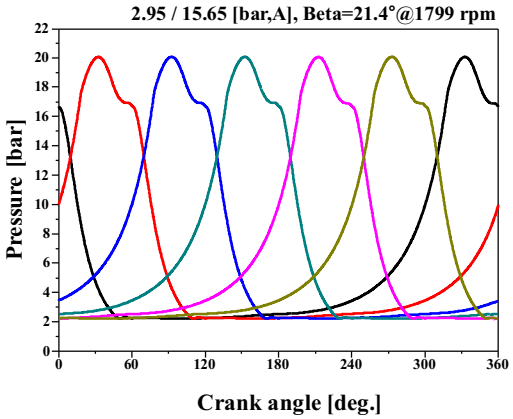

Figure 5: Cylinder pressure

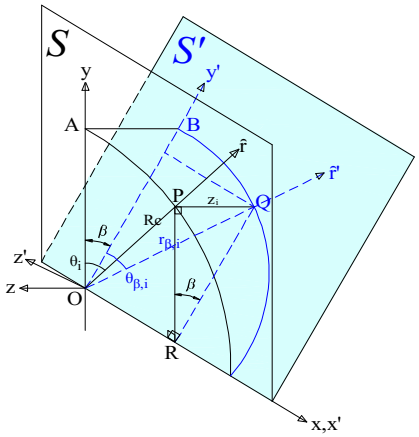

Figure 6: Coordinate system for swash plate

3.3 Swash plate dynamics

The coordinate system for the swash plate is shown in Fig. 6. S' is the plane of the swash plate, and S is the vertical plane. The swash plate inclination angle β is defined by the angle between S' and S. A piston located at A on the vertical axis is designated as piston no. 1. The swash plate rotates in the –z direction, and the crank angle θ=0° is defined by the swash plate angular position when piston no. 1 reaches the top dead center. If point Q represents the i^{th} piston location, then the crank angle of the i^{th} piston and the distance from the origin to the piston in the inclined plate are given by equations (6) and (7), respectively.

$$\theta_i = \frac{\pi}{3}(i-1) - \theta_c \quad , \quad r_{\beta,i} = R_c \cdot \sqrt{1+\cos^2\theta_i \cdot \tan^2\beta} \qquad (6),(7)$$

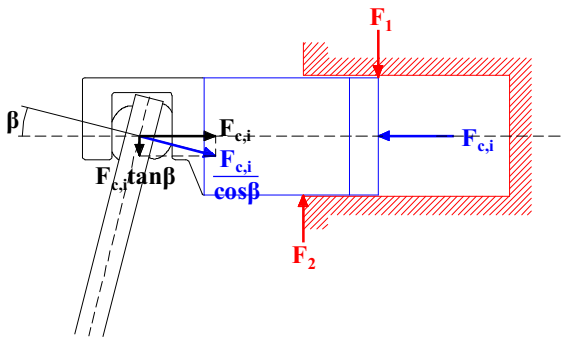

Figure 7: Forces acting on a piston

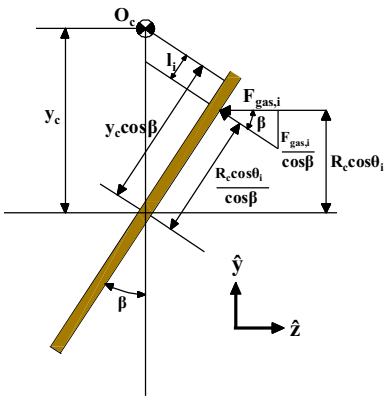

Figure 8: Forces and moments on swash plate

Fig.7 shows forces acting on a piston. $F_{c,i}$ is the combined force of cylinder gas pressure $F_{gas,i}$ and piston inertia $F_{iner,i}$ and $F_{c,i}/\cos\beta$ is the force exerted by the swash plate through piston shoe. $F_{1,i}$ and $F_{2,i}$ are forces acting on the piston side wall. These side forces can be obtained by force and moment balance on the piston. These forces are written as in equations (8)-(11).

$$F_{gas,i} = A_p \cdot P_{c,i}(\theta_i) \quad , \quad F_{iner,i} = -(m_p + 2m_{shoe})\ddot{z}_p \tag{8),(9)}$$

$$F_{1,i} = F_{2,i} + F_{c,i} \tan\beta \quad , \quad F_{2,i} = \frac{(l_p + z_i - l_c) \cdot F_{c,i} \tan\beta}{l_c - z_i} \tag{10),(11)}$$

Fig.8 shows various forces and moments acting on the swash plate. The swash plate bush is allowed to slide along the crankshaft, while it is to be rotated at around the plate lug hinge. F_{st} is the force of the coil spring situated the right side of the swash plate bush. F_{cr} and F_{re} are the forces due to the crank room pressure and coil spring on the left side of the swash plate bush, respectively. M_{gas}, M_{iner}, M_{st} are the moments produced by F_{gas}, F_{iner}, and F_{st}, respectively, as in equations (12)-(14).

$$M_{gas,i} = \frac{F_{gas,i}}{\cos\beta} \cdot l_i \quad , \quad M_{iner,i} = \frac{F_{iner,i}}{\cos\beta} \cdot l_i \quad , \quad M_{st,i} = F_{st} \cdot y_c \tag{12),(13),(14)}$$

where l_i and y_c are the distances of related forces to the moment center as shown in Fig.8. The moment center, or the rotation center of the swash plate is indicated by 'O_c' which is the interception of the vertical line passing through the bush center and the normal line from hinge center of the lug.
The moment arm l_i due to the i^{th} cylinder gas force is obtained as in equation (15) .

$$l_i = y_c \cos\beta - \frac{R_c \cos\theta_i}{\cos\beta} \tag{15}$$

M_{cr} and M_{re} are the moments by F_{cr} and F_{re}, respectively. M_{cent} is the moment due to centrifugal force of the swash plate itself. These are given by equations (16)-(18)

$$M_{cr} = y_c \cdot n_c A_p P_{cr} \quad , \quad M_{re} = F_{re} \cdot y_c \quad , \quad M_{cent} = F_{cent} \cdot z_{cent} \tag{16),(17),(18)}$$

Sum of the moments in the direction of increasing the swash plate inclination and opposite one are given by equations (19) and (20), respectively.

$$M^+ = \sum (M_{gas,i} + M_{iner,i}) + M_{st} \quad , \quad M^- = M_{cr} + M_{re} + M_{cent} \tag{19),(20)}$$

Yawing moment on the swash plate and shaft driving torque T_z are given by equations (21) and (22), respectively.

$$T_z^{'} = \sum_{i=1}^{6} (r_{\beta,i} \sin\theta_{\beta,i} \cdot F_{c,i} \sin\beta + r_{\beta,i} \frac{\mu_s F_{c,i}}{\cos\beta}) \quad , \quad T_z = \frac{T_z^{'}}{\cos\beta} \tag{21),(22)}$$

Torque load to run the compressor is expressed by equation (23).

$$T_L = T_z + T_B + T_{TH} \tag{23}$$

where T_B is the torque load due to shaft bearing friction, and T_{TH} is the torque load due to thrust bearing friction.
Mechanical loss is the total sum of the friction losses at the piston side forces, piston shoes, shaft bearings, and thrust bearing, as given by equation (24).

$$L_{mech} = L_p + L_{shoe} + L_B + L_{thrust} \tag{24}$$

where L_p, L_{shoe}, L_B, and L_{thrust} are given by equations (25)-(28),respectively.

$$L_p = \sum_{i=1}^{6} \mu_p \left|\dot{z}_p\right| \cdot \left(\left|F_{1,i}\right| + \left|F_{2,i}\right|\right) \quad , \quad L_{shoe} = \sum_{i=1}^{6} r_{\beta,i} \cdot \omega \cdot \mu_{shoe} \cdot \frac{F_{c,i}}{\cos\beta} \qquad (25),(26)$$

$$L_B = \omega \cdot r_{sh} \cdot f_{B1} \cdot F_{B1} + \omega \cdot r_{sh} \cdot f_{B2} \cdot F_{B2} + \omega \cdot r_{SB} \cdot f_{SB} \cdot F_{SB} \qquad (27)$$

$$L_{thrust} = \omega \cdot R_{needle} \cdot \mu_{thrust} \cdot \left(\sum_{i=1}^{6} F_{c,i} + F_{RE}\right) \qquad (28)$$

The compressor work, W_c, is the sum of the gas compression work and total mechanical loss.

4. Calculation results and discussion

4.1 Experimental validation

For the validation of the simulation program, calculation results of mass flow rates $\dot{m}_d$, cooling capacity Q_c, compressor work W_c, and COP were compared to experimental data measured in a compressor calorimeter as shown in Fig. 9(a)–(d).

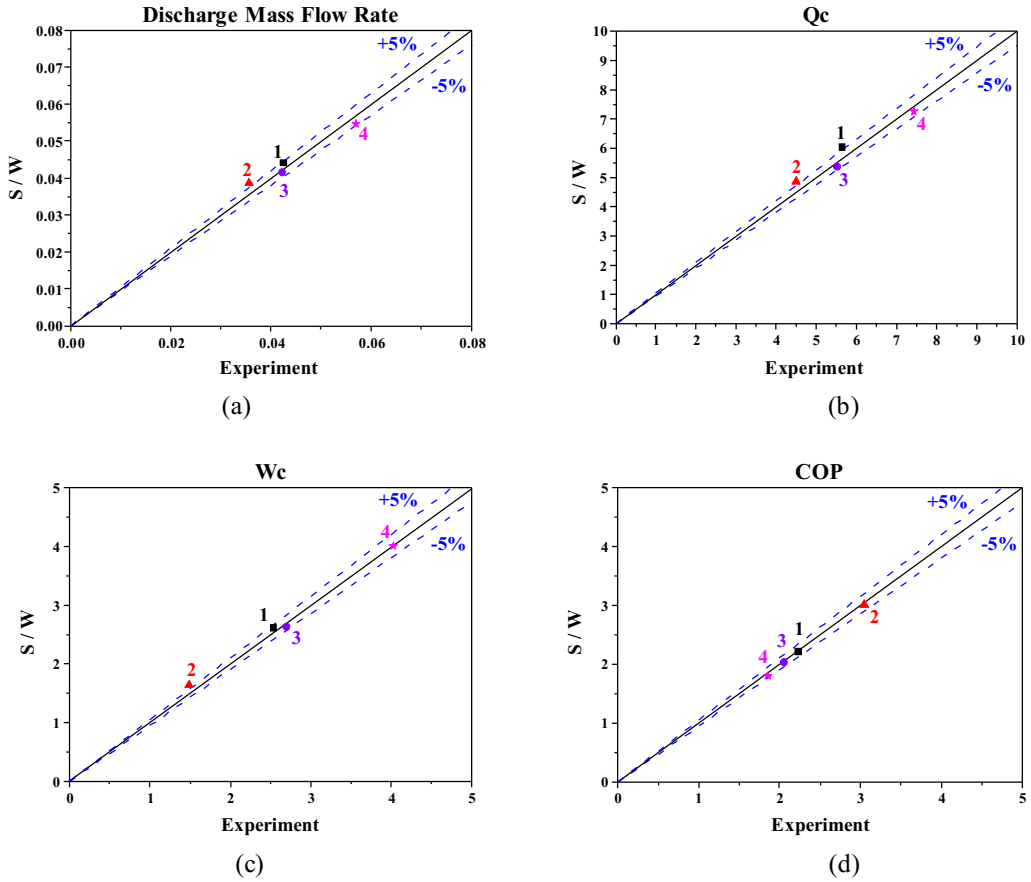

Figure 9: Simulation results vs. experimental data :

(a) mass flow rate, (b) cooling capacity, (c) compressor input, (d) COP

The compressor operating conditions for measurements are listed in Table 2. Except for the data of case 2, where compressor operating speed was the lowest among the four cases, all data of the mass flow rate, cooling capacity, compressor input, and COP showed a marginally good comparison between calculations and experiments within ±5% error range. For case 2, mass flow rate was calculated 8.9% larger than experimental data, resulting in larger calculation values for the cooling capacity and compressor input. For discharge gas temperature, calculation results compare well with experimental data as shown in Fig.10.

Table 2: Operating conditions for measurements

	CASE #1	CASE #2	CASE #3	CASE #4
Ps [bar, A]	2.95	4.97	2.79	2.806
Pd [bar, A]	15.65	19.99	16.03	15.94
Ts [°C]	10.33	25.9	8.85	9.0
RPM	1799	796	1999	3000

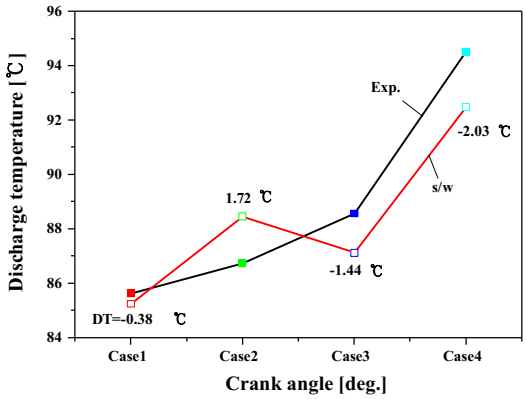

Figure 10: Discharge temperature: Exp. vs. s/w

4.2 Variable capacity operation

Fig.11 show the crank room pressure P_{cr} variation with β. At β=21.4°, calculation of P_{cr} agrees quite well with measurement value. Fig.12 shows PV diagrams at different swash plate angles. With decreasing β, PV diagram becomes narrower because piston stroke decreases and also clearance volume increases at the same time. Increased clearance volume expands further during the expansion process, causing delay in the start of the suction process.

As illustrated in Fig.13(a)(b), the volumetric efficiency, cooling capacity, and compressor input decrease with decreasing β. COP, the ratio of Q_c to W_c, is more or less constant for β >14°, but drops rapidly for smaller β.

Compressor efficiencies were calculated at various β, and presented in Fig.13(b). Adiabatic efficiency η_{ad} shows a peak near β=14°, while mechanical efficiency η_{mech} decreases with decreasing β. Since adiabatic efficiency η_{ad} is equivalent to the ratio of area between the two constant pressure (P_d and P_s) lines to the total area in PV diagram as in Fig.12, it is mainly affected by over and under compression losses, which in turn are related to valve opening behavior for given flow rate. For this particular compressor configuration, best result was found at β=14°. The reason why the mechanical efficiency decreases with decreasing β is that gas force in cylinder does not change much with decreasing β so the friction force at piston shoe becomes relatively large compared to compression work which decreases with decreasing β. Consequently, compressor total efficiency $\eta_c(=\eta_{ad}\cdot\eta_{mech})$ is more or less constant for β >14°, and it decreases with decreasing β below 14°, whose trend is similar to that of COP as in Fig.9(d).

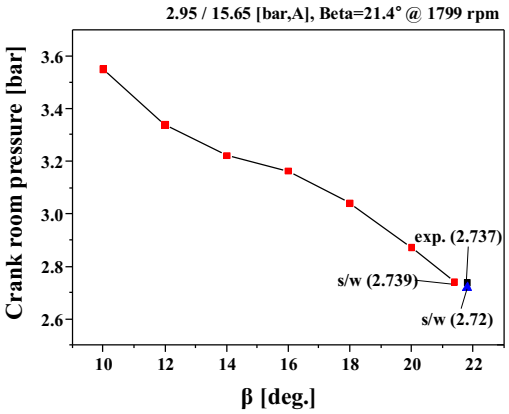

Figure 11: Crank room pressure vs. β

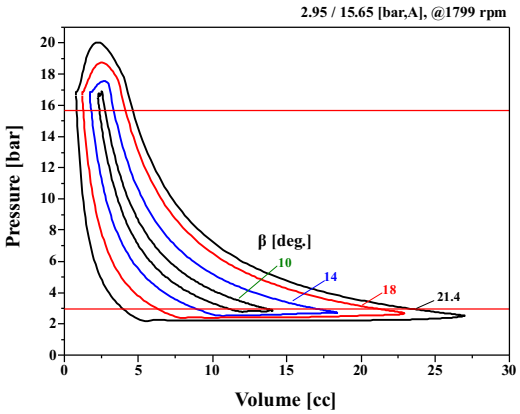

Figure 12: P-V diagram at various β

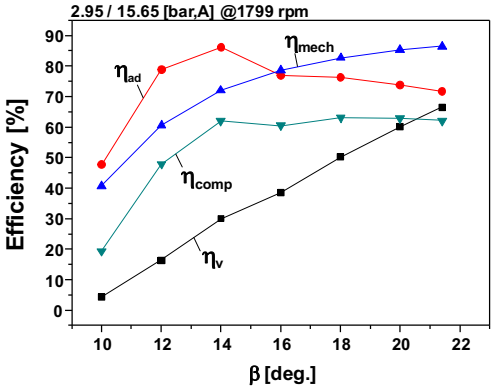

(a)

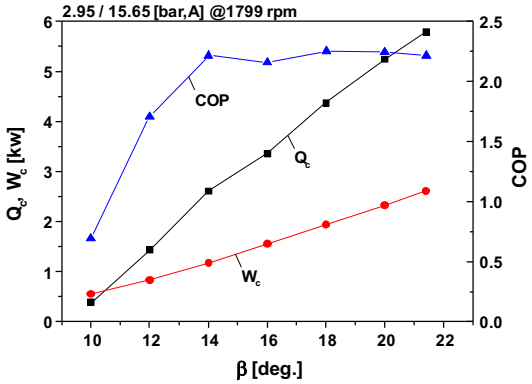

(b)

Figure 13: Effects of the swash plate angle β on the compressor performance

5. Conclusion

- Numerical analysis was carried out to estimate the performance of a variable capacity swash plate compressor.
- For validation of the numerical analysis, simulation data was compared to experimental data of a compressor calorimeter under four different operating conditions. Mass flow rate, compressor input, and COP were well compared within ±5% error range, except for the operating condition where the compressor speed was the lowest.
- By using the simulation program, variations in the compressor performance such as capacity, input power, crank room pressure, and various compressor efficiencies in accordance with changes in the swash plate inclination could be estimated.

NOMENCLATURE

A	area	(m^2)
f	friction coefficient	(-)
F	force	(N)
l	distance	(m)
L	loss	(W)
M	mass, moment	(kg, N·m)

$\dot{m}$	mass flow rate	(kg/s)
P	pressure	(bar)
r	radius	(m)
R_c	swash plate radius in S-plane	(m)
T	temperature, torque	(°, N·m)
t	time	(s)
V	volume	(m^3)
$\dot{z}_p$	piston velocity	(m/s)
$\ddot{z}_p$	piston acceleration	(m/s^2)
θ	crank angle	(°)
μ	friction coefficient	(-)
ρ	density	(kg/m^3)
ω	angular velocity	(rad/s)
Subscript		
B	bearing	
c	cylinder	
dv	discharge valve	
lk	leakage	
sh	shaft	
sv	suction valve	

REFERENCES

[1] K. Tojo, K. Takao, M. Ito, et al., Dynamic behavior of variable displacement compressor for automotive air conditioners, SAE Trans 99 (6) (1990) 40-48
[2] Y. Liu, G. Hui, Motion simulation and dynamic analysis of a four-cylinder wobble-plate compressor, Proceedings of 2012 International Conference on Mechanical Engineering and Material Science (2012) [paper 437]
[3] N. Ishii, Y. Abe, T. Taguchi, et al., Dynamic behavior of variable displacement wobble plate compressor for automotive air conditioners, Proceedings of the 1990 International Compressor Engineering Conference at Purdue, USA (1990) 345-53
[4] K. Yoshida, K. Kasahara, S. Watanabe, Dynamic behavior of variable stroke swash plate mechanism, Journal of System Design and Dynamics (2008) 561-71
[5] C.Q. Tian, Y.F. Liao, X.T. Li, A mathematical model of variable displacement swash plate compressor for automotive air conditioning system, International Journal of Refrigeration 29 (2006) 270-280
[6] C.Q. Tian, H.B. Xu, X.T. Li, Y.F. Liao, Simulation and performance analysis of control mechanism in variable displacement swash plate compressor, Applied Thermal Engineering 27 (2007) 1868-1875
[7] G.H. Lee, T.J. Lee, A study on the variable displacement mechanism of swash plate type compressor for automotive air conditioning system, Proceedings of the 2004 International Compressor Engineering Conference at Purdue, USA (2004) [paper 1706]
[8] J.F. Below, D.A. Miloslavich, Dynamics of the swash plate mechanism, Proceedings of the 1984 International Compressor Engineering Conference at Purdue, USA (1984) [paper 437]
[9] R.K. Jha, S. Muthu, S. Sivakumar, Design methodology and dynamic simulation of fixed displacement swash plate compressor, ICoRD'15 – Research into Design Across Boundaries 2 (2015) 545-557
[12] H.J. Kim, G.H. Lee, J.H. Yoo, A numerical study on the performance analysis of swash plate compressor for automotive air conditioners, The Society of Air-Conditioning and Refrigerating Engineers of Korea (1997) 497-502
[13] G.H. Lee, H.J. Kim, T.J. Kim, J.H. Yoo, A numerical method on the efficiency prediction of swash plate compressor for automotive air conditioner, The Society of Air-Conditioning and Refrigerating Engineers of Korea (1998) 1102-1107